Journal of Materials Chemistry B

PAPER

View Article Online
View Journal

Cite this: DOI: 10.1039/c8tb02864h

Development of a near-infrared ratiometric fluorescent probe for glutathione using an intramolecular charge transfer signaling mechanism and its bioimaging application in living cells†

Yong Zhou,[a] Li Zhang,[a] Xuan Zhang *[ab] and Zhi-Jia Zhu[a]

Received 30th October 2018,
Accepted 22nd December 2018

DOI: 10.1039/c8tb02864h

rsc.li/materials-b

A novel near-infrared (NIR) ratiometric fluorescent probe **HBT-GSH** derived from conjugated benzothiazole was developed for the selective detection of glutathione (GSH) over cysteine (Cys) and homocysteine (Hcy). The probe was sophisticatedly designed based on the GSH selectively induced enhancement of intramolecular charge transfer (ICT) fluorescence. It was synthesized by masking the active phenol group of 2,6-bis(2-vinylbenzothiazolyl)-4-fluorophenol through an acetyl group that acts both as a trigger of the ICT fluorescence and as a recognition moiety for GSH. On its own, the probe **HBT-GSH** exhibited strong blue fluorescence emission at 426 nm and weak NIR fluorescence emission at 665 nm in aqueous solution, whereas the NIR fluorescence was significantly enhanced and the short emission decreased upon the addition of GSH. Thus an NIR ratiometric fluorescent probe for GSH was developed based on the GSH-selective removal of the acetyl group, therefore switching on the ICT in **HBT-GSH**. The fluorescence intensity ratio ($I_{665\,nm}/I_{426\,nm}$) showed a linear relationship with a GSH concentration of 0–100 μM with a detection limit of 0.35 μM. Moreover, the fluorescent probe was successfully used for the ratiometric fluorescence bioimaging of GSH in living cells.

Introduction

Glutathione (GSH) is one of the most important intracellular biothiols that play crucial roles in many physiological processes, such as the maintenance of redox homeostasis, intracellular signal transduction and gene regulation.[1–3] As the most abundant non-protein thiol, the normal GSH concentration ranges from 1 to 15 mM in various cells,[4] while abnormal GSH levels could be related to some diseases, such as cancer, Alzheimer's, and lung and cardiac diseases.[5–8] Thus the development of a novel strategy for quantitatively monitoring the intracellular GSH level will be very helpful for the early diagnosis and treatment of related diseases.

The design and synthesis of small molecule-based fluorescent probes is one of the most promising methods for intracellular GSH detection due to the many merits of fluorescence analysis, such as high sensitivity and selectivity, bioimaging *in vivo*, and non-invasiveness.[9–27] However, it is still a challenge to discriminate GSH from cysteine (Cys) and homocysteine (Hcy) due to their similar molecular structures and reactivity.[28–35] Furthermore, probes with near-infrared (NIR, 650–900 nm) fluorescence emission have attracted increasing attention due to their characteristic advantages, such as deeper tissue penetration and minimum interference from the indigenous auto-fluorescence of the biosystem background.[23–27,36] Additionally, ratiometric fluorescent probes could provide an inherent reliability originating from their advantage of effective self-calibration by monitoring two well-resolved emissions.[37] To date, some ratiometric fluorescent probes for GSH have been reported,[38–46] but only a few of them have shown fluorescence emission in the NIR region.[45,46] Therefore, the development of an NIR ratiometric fluorescent probe for intracellular GSH-selective detection is a more promising but still challenging task.

Recently, we have found that π-conjugated extended benzothiazole derivatives exhibit NIR emission in a polar solvent, originating from the deprotonation of the phenol group

[a] Key Laboratory of Science and Technology of Eco-Textiles, Ministry of Education, College of Chemistry, Chemical Engineering and Biotechnology, Donghua University, Shanghai 201620, China. E-mail: xzhang@dhu.edu.cn
[b] State Key Laboratory of Fine Chemicals, Dalian University of Technology, Dalian 116024, China

† Electronic supplementary information (ESI) available: Absorption titration spectra, ^{1}H NMR, ^{13}C NMR, and MALDI-TOF-MS spectra of related compounds, and mass spectra of the probe **HBT-GSH** in the absence and presence of GSH. See DOI: 10.1039/c8tb02864h

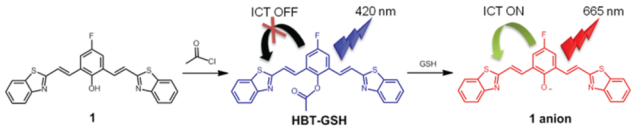

Scheme 1 Synthesis of **HBT-GSH** and the proposed signaling mechanism for GSH detection.

switching on an intramolecular charge transfer (ICT) process.[47] In this work, we have developed a novel NIR ratiometric fluorescent probe **HBT-GSH** (Scheme 1) based on a conjugated benzothiazole framework, where the active phenol group was masked with an acetyl group that acts both as a trigger of the ICT fluorescence and as a recognition moiety for GSH. The probe showed a strong short-wavelength fluorescence emission at 426 nm that decreased and an ICT fluorescence emission at 665 nm that increased upon addition of GSH, making NIR ratiometric fluorescence analysis available. Furthermore, the probe **HBT-GSH** could distinguish GSH well from Cys/Hcy in aqueous solution and be successfully applied in imaging of living cells.

Results and discussion

Design and synthesis

π-Conjugated extended benzothiazole derivatives exhibit ICT fluorescence emission in the NIR range with a high quantum yield and a large Stokes shift, making them promising for the development of NIR fluorescent probes by masking their active phenol group.[47] Benzothiazole derivative **1** was firstly synthesized by following a similar procedure to that established previously,[47] and then the probe **HBT-GSH** was easily afforded by treating **1** with acetyl chloride in acetone, as shown in Scheme 1. The chemical structure of the probe **HBT-GSH** was confirmed by ^{1}H NMR, ^{13}C NMR, and MALDI-TOF-MS, elemental analysis, and the synthesis details are presented in the Experimental section.

Selectivity toward GSH

Compound **1** showed a short-wavelength emission at 426 nm in $CHCl_3$ but an NIR emission at 688 nm in DMSO (Fig. S1, ESI†), due to the switching on of an ICT process in the latter polar solvent.[47] This allowed conjugated benzothiazole derivative **1** to be a suitable platform to construct the NIR fluorescent probe **HBT-GSH**. To examine the selectivity of probe **HBT-GSH** toward GSH, the fluorescence and absorption spectra were measured in the presence of 10 equiv. of various species such as common amino acids (GSH, Cys, Hcy, Asp, Asn, Ser, Pro, Ala, Gly, Val, Leu, lle, Thr, Arg, Glu, Gln, Tyr, His, Met, Phe, Trp, Lys, Tau), cations (Na^+, K^+, Ca^{2+}, Mg^{2+}), anions (SO_4^{2-}, NO_3^-, CO_3^{2-}, Cl^-), Na_2S and glucose, respectively (Fig. 1). As shown in Fig. 1a, the probe **HBT-GSH** only showed a short wavelength fluorescence at 426 nm, but the addition of GSH strongly enhanced the NIR fluorescence at 665 nm accompanied by a decrease in blue emission at 426 nm. The fluorescence quantum yields were measured to be 0.138 and 0.245 in the absence and presence of GSH, respectively. While Cys and Hcy induced a moderate increase in NIR fluorescence, other species did not make a

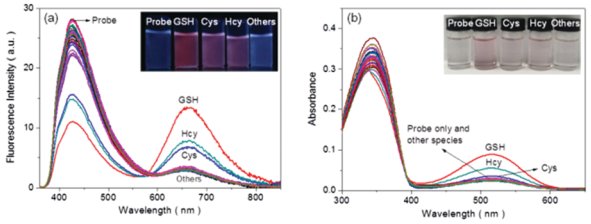

Fig. 1 Fluorescence (a) and absorption (b) spectra of **HBT-GSH** in the absence and presence of 10 equiv. of various amino acids and biologically relevant species in aqueous PBS buffer (pH = 7.4). Insets are the fluorescence (a) and solution (b) color change of the probe in the presence of GSH, Cys, Hcy and other species tested in this work, where the fluorescence in (a) was obtained by exposure to a UV lamp at 365 nm. The excitation wavelength is 350 nm for fluorescence measurement.

noticeable change in NIR fluorescence emission at 665 nm. A fluorescence color change from blue to red was clearly observed in the presence of GSH (Fig. 1a). This indicates that the probe **HBT-GSH** exhibited a high selectivity toward GSH in aqueous solution. Meanwhile, the absorption intensity at 516 nm showed a large increase in the presence of GSH accompanied by a color change from colorless to red (Fig. 1b), suggesting the availability of a naked-eye detection of GSH. In addition, the ratios of two emission intensities ($I_{665\,nm}/I_{426\,nm}$) clearly showed significant enhancement in the presence of GSH over Cys/Hcy and other species, and the existence of these species did not cause substantial interference to GSH detection (Fig. S2, ESI†).

The time-dependent fluorescence response of the probe **HBT-GSH** in the presence of 10 equiv. of GSH and Cys/Hcy was also performed, respectively. As shown in Fig. 2a, the NIR fluorescence intensity at 665 nm increased continuously and reached equilibrium at about 120 min for GSH, but slower reaction kinetics were observed for Cys/Hcy, demonstrating the high selectivity of the probe **HBT-GSH** toward GSH. The probe **HBT-GSH** displayed no noticeable changes in NIR fluorescence in the absence of GSH, suggesting that the probe is stable enough under experimental conditions.

Ratiometric fluorescence determination of GSH

The change in fluorescence character of the probe **HBT-GSH** means it is possible to develop it as a ratiometric probe for GSH. Firstly, the influence of pH on the fluorescence of the probe in the absence and presence of GSH were investigated over the range of pH 2–10. Without GSH, the fluorescence intensities ratio displayed negligible changes at pH < 8 but increased

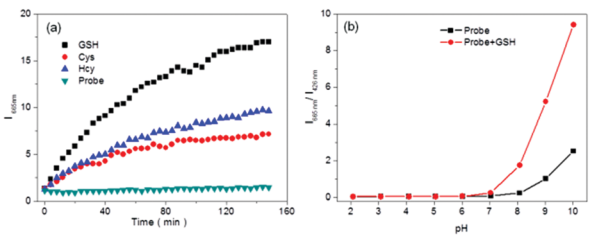

Fig. 2 Effect of time and pH on fluorescence intensity of **HBT-GSH** in the absence and presence of various biothiols.

obviously after that (Fig. 2b), revealing that partial hydrolysis of the probe could occur under the condition pH > 8. In the presence of GSH, while the $I_{665\,nm}/I_{426\,nm}$ ratio showed almost no change at pH < 6, a noticeable increase appeared at pH > 6 and the ratio was significantly enhanced under pH > 8 (Fig. 2b), suggesting that the GSH-induced removal of the acetyl group in the probe **HBT-GSH** was facilitated under basic conditions. Then the ratiometric fluorescence titrations were performed at the physiological pH 7.4 in the phosphate buffer solution (10 mM, 50% DMSO). As shown in Fig. 3a, the fluorescence emission gradually decreased at 426 nm and increased at 665 nm with increasing amounts of GSH up to 180 μM. The $I_{665\,nm}/I_{426\,nm}$ intensity ratios were found to follow a good linear relationship (R^2 = 0.9968) with a GSH concentration ranging from 0 to 100 μM (Fig. 3b). The detection limit was estimated to be 0.35 μM according to S/N = 3. Hence, the probe **HBT-GSH** could detect GSH quantitatively by a ratiometric fluorescence method with excellent sensitivity. In addition, the absorption titration showed that the peak at 516 nm gradually increased upon the addition of GSH and the solution color became red (Fig. S3, ESI†).

Sensing mechanism

To confirm that probe **HBT-GSH** has been transformed into **1** in the presence of GSH, as shown in Scheme 1, MALDI-TOF-MS mass analysis of a mixed solution of the probe with 10 equiv. of GSH was conducted. A prominent peak at m/z = 453.1 corresponding to $[\mathbf{1} + Na]^+$ was observed, providing solid evidence for the fact that GSH induced the cleavage of the acetyl moiety in probe **HBT-GSH** (Fig. S4, ESI†). The high selectivity toward GSH over Cys/Hcy has usually been considered from the point of view of their structural differences, where GSH has a longer flexible backbone that could provide the additional chance to form some intermolecular interactions with the probe, such as hydrogen bonds and electrostatic interactions.[18,23,26] Accordingly, we speculated that the benzothiazole units in the probe **HBT-GSH** could be involved in hydrogen bond interactions with carboxylic acid groups in biothiols. Only GSH has a much better match distance between HS and the terminal COOH groups (the HS–COOH separation for Cys is 3 bonds, that for Hcy is 4 bonds, and that for GSH is 6/8 bonds) and two carboxylic acid groups that were favourable to the formation of hydrogen bonds. The reaction kinetics showed the order of GSH > Hcy > Cys (Fig. 2a) that matched well with the distance between HS and the terminal COOH groups in these biothiols. This suggested that such possible hydrogen bonding interactions might therefore promote the cleavage reaction rate of GSH toward the acetyl moiety in probe **HBT-GSH**. A DFT calculation based on the Gaussian 09 program was further performed to gain better insights into the NIR fluorescence and signaling mechanism. Fig. 4 presents the optimized ground state structures of both the probe **HBT-GSH** and the anion of **1**. It revealed that the π electrons of the probe **HBT-GSH** were well delocalized over the whole molecular skeleton on both the lowest unoccupied molecular orbital (LUMO) and the highest occupied molecular orbital (HOMO). However, the π electrons of the **1** anion were mainly localized on the phenolate group on the HOMO, and delocalized over the whole molecular skeleton on the LUMO, suggesting the occurrence of an ICT process from the phenolate donor to the benzothiazole acceptor. The phenol moiety has been known to be a latent electron donor but acts as a strong electron donor when it is transformed into a phenolate, and could therefore switch on an ICT emission.[47,48] Based on the TD-DFT calculation on the excited state, the fluorescence emission wavelengths were predicted to be 420 nm and 670 nm for the probe **HBT-GSH** and **1** anion, respectively. The good reproduction of the experimental results implied the reliability of the present theoretical calculation level. Thus the signaling mechanism could be rationalized by GSH-induced removal of the acetyl group and switching-on of ICT, as shown in Scheme 1.

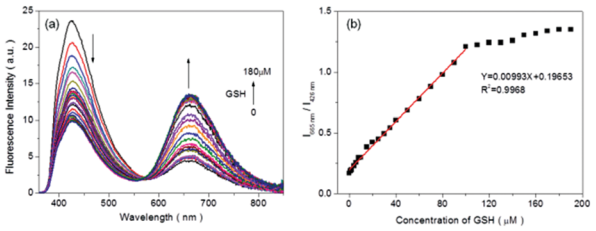

Fig. 3 Change in fluorescence spectra of **HBT-GSH** (10 μM) with the addition of various amounts of GSH (0–180 μM) (a). The corresponding linear relationship between the fluorescence intensity ratio ($I_{665\,nm}/I_{426\,nm}$) and the concentration of GSH (0–100 μM) (b).

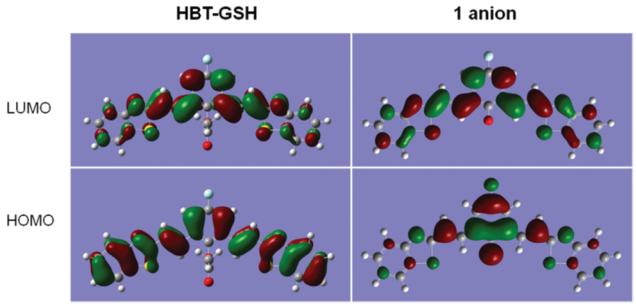

Fig. 4 LUMO and HOMO orbitals of **HBT-GSH** and anion of **1** in the ground state.

Fluorescence imaging in living cells

To evaluate the potential practical applications of probe **HBT-GSH**, the fluorescence imaging of GSH in living HeLa cells was also performed. Firstly, the cytotoxicity of probe **HBT-GSH** was evaluated by a CCK-8 assay. The results showed that high cell viability remained even after treatment with 40 μM of probe at 37 °C for 24 h (Fig. S5, ESI†), which suggested the low cytotoxicity of the probe **HBT-GSH** and its potential in the imaging of live cells. Thus 20 μM of the probe **HBT-GSH** was used for bioimaging of GSH in living HeLa cells with a Leica TCS SP8 microscope, where dual blue and red channels were monitored upon excitation at 405 nm and 552 nm respectively (Fig. 5). When HeLa cells were incubated with the probe **HBT-GSH** (20 μM) for 60 min at 37 °C, both blue and red fluorescence emissions were observed in the two channels (Fig. 5b and c),

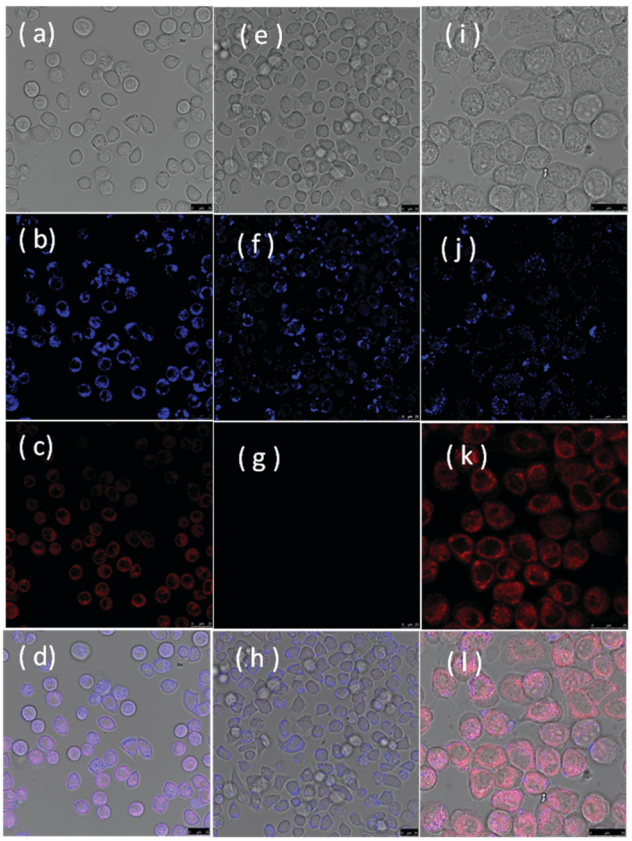

Fig. 5 Confocal fluorescence images of living HeLa cells incubated with the probe **HBT-GSH** (20 μM) for 60 min at 37 °C: cells without treatment (a–d), cells with pre-treatment by NEM (1 mM) (e–h), and cells with pre-treatment by NEM (1 mM) and the further addition of 200 μM GSH (i–l). (a, e and i) are the bright-field images; (b, f and g) and (c, g and k) are the fluorescence images at blue and red channels, respectively; (d, h and l) are the overlap of the fluorescence and bright-field images.

where the NIR emission resulted from the intracellular GSH-induced removal of the acetyl group in the probe. In the control experiment, HeLa cells were pretreated with *N*-ethylmaleimide (NEM, a known scavenger for GSH, 1 mM for 60 min), and thereafter incubated with probe **HBT-GSH** (20 μM) for another 60 min. As shown in Fig. 5f and g, while the blue fluorescence remained, there was no fluorescence in the red channel. Then the NEM-pretreated HeLa cells were further sequentially incubated with GSH (200 μM) for 30 min, and the probe **HBT-GSH** (20 μM) for 60 min at 37 °C. A bright fluorescence in the red channel was again observed inside the cells (Fig. 5k) accompanied by a weak fluorescence in the blue channel (Fig. 5j). The above results suggested that probe **HBT-GSH** can be used as a promising fluorescent probe for GSH imaging in living cells.

Conclusions

In summary, a novel NIR ratiometric fluorescent probe **HBT-GSH** was developed for the selective detection of GSH over Cys and Hcy in aqueous solution. The probe was synthesized by masking the active phenol group of 2,6-bis(2-vinylbenzothiazolyl)-4-fluorophenol through an acetyl group that acts both as a trigger of ICT fluorescence and as a recognition moiety for GSH. Based on mass analysis and DFT calculations, the signaling mechanism of the GSH-induced removal of the acetyl group and the switching on of the ICT fluorescence was proposed. The fluorescence intensity ratio ($I_{665\,nm}/I_{426\,nm}$) showed a linear relationship with a GSH concentration of 0–100 μM with a detection limit of 0.35 μM. Moreover, the probe had low cytotoxicity and was successfully used for the ratiometric fluorescence bioimaging of GSH in living cells.

Experimental

Materials and methods

All the chemicals are analytical grade and purchased from Sinopharm Chemical Reagents Corp. (Shanghai, China). Phosphate buffered saline (PBS, pH = 7.4) was prepared from K_2HPO_4 (0.1 M) and KH_2PO_4 (0.1 M). A stock solution of the probe **HBT-GSH** was prepared in DMSO and all the other species solutions were prepared in deionized water. ^{1}H NMR and ^{13}C NMR spectra were recorded on a Bruker AVANCE III 400 MHz spectrometer. Mass spectra were obtained on an AB Sciex MALDI-TOF/TOF™ MS. Fluorescence spectra were measured on an Edinburgh FS5 spectrofluorometer with Ex/Em slit widths of 5 nm. Absorption spectra were obtained on a SHIMADZU UV-1800 spectrophotometer. Confocal fluorescence imaging experiments in living HeLa cells were carried out with a Leica TCS SP8 microscope.

Theoretical calculations were performed based on the Gaussian 09 package.[49] The ground state and the first singlet excited state geometries of the compounds were optimized in the gas phase using density functional theory (DFT) and time-dependent density functional theory (TDDFT) at the B3LYP/6-31+G(d) level, respectively. The fluorescence emission properties were calculated using TDDFT based on the optimized first singlet excited state geometries, respectively.

Synthesis

Synthesis of 2,6-diformyl-4-fluorophenol. The available procedures were followed in a similar way to previous work.[47,50] Briefly, under an N_2 atmosphere, 4-fluorophenol (5 mmol) and hexamethylenetetramine (15 mmol) were dissolved in TFA (8 mL) and refluxed at 110 °C for 90 h. The mixture was then cooled down to room temperature and poured into a 0.8 M HCl solution (60 mL), and the 2,6-diformyl-4-fluorophenol was obtained by filtration. Yield: 48%. ^{1}H NMR (400 MHz, $CDCl_3$), δ (ppm): 11.38 (s, 1H), 10.22 (s, 2H), 7.69 (d, J = 4 Hz, 2H). ^{13}C NMR (100 MHz, DMSO-d_6), δ (ppm): 190.87, 190.85, 158.46, 158.45, 156.17, 153.78, 125.06, 125.01, 122.43, 122.20.

Synthesis of 1. Under an N_2 atmosphere, 2,6-diformyl-4-fluorophenol (1 mmol) and 2-methylbenzothiazole (4 mmol) were refluxed in acetic anhydride (2 mL) for 48 h. After cooling to room temperature, the solid was obtained by filtration and thoroughly washed with water. The obtained solid was further dissolved in pyridine (8 mL) and refluxed at 115 °C for 1 h, then water (8 mL) was added and it was stirred at 100 °C for another 4 h. After cooling down to room temperature, the crude product

was collected by filtration and purified by washing with CH_2Cl_2 to give **1** as a yellow solid. Yield: 33%. ^{1}H NMR (400 MHz, DMSO-d_6), δ (ppm): 9.98 (s, 1H), 8.13 (d, J = 8 Hz, 2H), 8.00 (t, J = 8 Hz, 4H), 7.77 (d, J = 8 Hz, 2H), 7.71 (d, J = 16 Hz, 2H), 7.56 (t, J = 8 Hz, 2H), 7.48 (t, J = 8 Hz, 2H); ^{13}C NMR (100 MHz, DMSO-d_6), δ (ppm): 166.47, 153.48, 150.11, 134.11, 131.20, 126.57, 125.51, 123.21, 122.61, 122.21, 114.07, 113.83. MALDI-TOF-MS: m/z calcd for $C_{24}H_{15}FN_2OS_2$, 430.53; found 431.01 $[M + H]^+$.

Synthesis of HBT-GSH. Compound **1** (0.1 mmol) was dissolved in acetone (100 mL) and acetyl chloride (0.15 mmol dissolved in 5 mL of acetone) was slowly added dropwise under stirring at 0 °C in the presence of Et_3N (0.2 mmol). After stirring at this temperature for 2 h, the mixture was warmed to room temperature and stirred for another 14 h. The reaction mixture was concentrated in a vacuum and the residue was dissolved in CH_2Cl_2 and then washed with water and brine, dried with $MgSO_4$; then the product was obtained by evaporation to dryness under reduced pressure. Yield: 79%. ^{1}H NMR (400 MHz, $CDCl_3$), δ (ppm): 8.04 (d, J = 8 Hz, 2H), 7.89 (d, J = 8 Hz, 2H), 7.52–7.37 (m, 5H), 2.54 (s, 3H). ^{13}C NMR (100 MHz, $CDCl_3$), δ (ppm): 169.00, 165.68, 161.79, 159.35, 153.86, 143.08, 134.52, 131.41, 131.33, 129.31, 129.29, 126.61, 126.02, 125.88, 123.40, 121.60, 114.07, 113.83, 20.62. MALDI-TOF-MS: m/z calcd for $C_{26}H_{17}FN_2O_2S_2$, 472.56; found 473.04 $[M + H]^+$. Elemental analysis: calcd for $C_{26}H_{17}FN_2O_2S_2 + H_2O$, C 63.65%, H 3.90%, N 5.71%; found: C 63.90%, H 3.57%, N 5.59%.

Cell imaging

HeLa cells were cultured in Dulbecco's Modified Eagle Medium (DMEM) supplemented with 10% fetal bovine serum at 37 °C in a 95% humidity atmosphere under 5% CO_2 environment. Then the cells were seeded in confocal microscope culture dishes with a density of 2×10^5 cells per well. The cells were then incubated with probe **HBT-GSH** (20 μM) for 60 min at 37 °C, and washed with PBS buffer (10 mM) three times to remove free probe. In the control experiments, the cells were pretreated with NEM (1 mM) for 60 min at 37 °C, followed by washing with PBS three times, and incubated with probe **HBT-GSH** (20 μM) for 60 min at 37 °C. In another control experiment, the cells were pretreated with NEM (1 mM) for 60 min at 37 °C, followed by washing with PBS three times, then incubated with GSH (200 μM) for 30 min, and further incubated with probe **HBT-GSH** (20 μM) for 60 min at 37 °C, respectively. All the cells were washed with PBS three times to remove free probe and then imaged in a Leica TCS SP8 microscope.

Cytotoxicity assay

The cytotoxicity of the probe to HeLa cells was evaluated with a Cell Counting Kit-8 (CCK-8) assay. In brief, HeLa cells were seeded in a 96-well plate (2×10^5 cells per well) and cultured at 37 °C for 24 h. Then, different concentrations of the probe **HBT-GSH** were added and incubated for 24 h. Finally, the CCK-8 reagent was added and the HeLa cells were incubated at 37 °C for another 4 h. The absorbance values of the wells were measured with a SpectraMax M3 microplate reader at 450 nm. The cell viability rate (VR) of the HeLa cells was calculated with the equation: VR = $A/A_0 \times 100\%$, where A_0 is the absorbance of the control group (*i.e.*, HeLa cells without the probe) and A is the absorbance of the experimental group (*i.e.*, HeLa cells treated with the probe). The cell survival rate from the control group was considered to be 100%.

Conflicts of interest

There are no conflicts to declare.

Acknowledgements

This work was financially supported by the State Key Laboratory of Fine Chemicals, Dalian University of Technology (KF 1715) and the Shanghai Municipal Natural Science Foundation (16ZR1401700). We would like to thank Dr Xiao-Juan Huang for her kind assistance with cell imaging experiments.

Notes and references

1 H. Chen, L. Zhou, C.-Y. Lin, M. C. Beattie, J. Liu and B. R. Zirkin, *Mol. Cell. Endocrinol.*, 2010, **323**, 147–154.
2 N. Akter, M. A. Sobahan, M. A. Hossain, M. Uraji, Y. Nakamura, I. C. Mori and Y. Murata, *Biosci., Biotechnol., Biochem.*, 2010, **74**, 2504–2506.
3 M. L. Reniere, A. T. Whiteley, K. L. Hamilton, S. M. John, P. Lauer, R. G. Brennan and D. A. Portnoy, *Nature*, 2015, **517**, 170–173.
4 J. H. Lee, A. Sharma, J. H. Jang, W. S. Shin, J. H. Lee and J. S. Kim, *J. Inclusion Phenom. Macrocyclic Chem.*, 2015, **82**, 117–122.
5 A. L. Ortega, S. Mena and J. M. Estrela, *Cancers*, 2011, **3**, 1285–1310.
6 T. Damy, M. Kirsch, L. Khouzami, P. Caramelle, P. L. Corvoisier, F. Roudot, J. L. Dubois, L. Hittinger, C. Pavoine and F. Pecker, *PLoS One*, 2009, **4**, 4871–4877.
7 S. K. Biswas and I. Rahman, *Mol. Aspects Med.*, 2009, **30**, 60–76.
8 C. B. Pocernich and D. A. Butterfield, *Biochim. Biophys. Acta*, 2012, **1822**, 625–630.
9 Q. Sun, D. Sun, L. Song, Z. Chen, W. Zhang and J. Qian, *Anal. Chem.*, 2016, **88**, 3400–3405.
10 L.-Y. Chen, J.-S. Park, D. Wu, C.-H. Kim and J. Yoon, *Sens. Actuators, B*, 2018, **262**, 306–312.
11 F. Chen, J. Zhang, W. Qu, X. Zhong, H. Liu, J. Ren, H. He, X. Zhang and S. Wang, *Sens. Actuators, B*, 2018, **266**, 528–533.
12 F. Chen, D. Han, H. Liu, S. Wang, K.-B. Li, S. Zhang and W. Shi, *Analyst*, 2018, **143**, 440–448.
13 G. Liu, X. Han, J. Zhang, Z. Xu, S. Liu, L. Zeng and J. Yin, *Dyes Pigm.*, 2018, **148**, 292–297.
14 X. Hou, X. Guo, B. Chen, C. Liu, F. Gao, J. Zhao and J. Wang, *Sens. Actuators, B*, 2015, **209**, 838–845.
15 L. Hu, X. Wei, J. Meng, X. Wang, X. Chen and J. Wang, *Sens. Actuators, B*, 2018, **268**, 264–269.

16 X. Ren, F. Wang, J. Lv, T. Wei, W. Zhang, Y. Wang and X. Chen, *Dyes Pigm.*, 2016, **129**, 156–162.
17 H. Zhou, J. Tang, L. Lv, N. Sun, J. Zhang, B. Chen, J. Mao, W. Zhang, J. Zhang and J. Zhou, *Analyst*, 2018, **143**, 2390–2396.
18 J. Zhang, X. Bao, J. Zhou, F. Peng, H. Ren, X. Dong and W. Zhao, *Biosens. Bioelectron.*, 2016, **85**, 164–170.
19 Q. Miao, Q. Li, Q. Yuan, L. Li, Z. Hai, S. Liu and G. Liang, *Anal. Chem.*, 2015, **87**, 3460–3466.
20 F. Wang, L. Zhou, C. Zhao, R. Wang, Q. Fei, S. Luo, Z. Guo, H. Tian and W.-H. Zhu, *Chem. Sci.*, 2015, **6**, 2584–2589.
21 G. Xu, Y. Tang and W. Lin, *New J. Chem.*, 2018, **42**, 12615–12620.
22 S.-Y. Lim, K.-H. Hong, D.-I. Kim, H. Kwon and H.-J. Kim, *J. Am. Chem. Soc.*, 2014, **136**, 7018–7025.
23 J. Yin, Y. Kwon, D. Kim, D. Lee, G. Kim, Y. Hu, J.-H. Ryu and J. Yoon, *J. Am. Chem. Soc.*, 2014, **136**, 5351–5358.
24 H.-J. Xiang, H. P. Tham, M. D. Nguyen, S. Z. F. Phua, W. Q. Lim, J.-G. Liu and Y. Zhao, *Chem. Commun.*, 2017, **53**, 5220–5223.
25 X. Xia, Y. Qian and B. Shen, *J. Mater. Chem. B*, 2018, **6**, 3023–3029.
26 C. Wang, X. Xia, J. Luo and Y. Qian, *Dyes Pigm.*, 2018, **152**, 85–92.
27 D. Lee, K. Jeong, X. Luo, G. Kim, Y. Yang, X. Chen, S. Kim and J. Yoon, *J. Mater. Chem. B*, 2018, **6**, 2541–2546.
28 S. Lee, J. Li, X. Zhou, J. Yin and J. Yoon, *Coord. Chem. Rev.*, 2018, **366**, 29–68.
29 L.-Y. Niu, Y.-Z. Chen, H.-R. Zheng, L.-Z. Wu, C.-H. Tung and Q.-Z. Yang, *Chem. Soc. Rev.*, 2015, **44**, 6143–6160.
30 C.-X. Yin, K.-M. Xiong, F.-J. Huo, J. C. Salamanca and R. M. Strongin, *Angew. Chem., Int. Ed.*, 2017, **56**, 13188–13198.
31 W.-W. Ma, M.-Y. Wang, D. Yin and X. Zhang, *Sens. Actuators, B*, 2017, **248**, 332–337.
32 Y. Tian, B. Zhu, W. Yang, J. Jing and X. Zhang, *Sens. Actuators, B*, 2018, **262**, 345–349.
33 X. Ren, H. Tian, L. Yang, L. He, Y. Geng, X. Liu and X. Song, *Sens. Actuators, B*, 2018, **273**, 1170–1178.
34 J.-Y. Xie, C.-Y. Li, Y.-F. Li, J. Fei, F. Xu, J. Ou-Yang and J. Liu, *Anal. Chem.*, 2016, **88**, 9746–9752.
35 J. Ou-Yang, C.-Y. Li, Y.-F. Li, J. Fei, F. Xu and S.-Y. Li, *Sens. Actuators, B*, 2017, **240**, 1165–1173.
36 Z. Guo, S. Park, J. Yoon and I. Shin, *Chem. Soc. Rev.*, 2014, **43**, 16–29.
37 M. H. Lee, J. S. Kim and J. L. Sessler, *Chem. Soc. Rev.*, 2015, **44**, 4185–4191.
38 Z. Liu, X. Zhou, Y. Miao, Y. Hu, N. Kwon, X. Wu and J. Yoon, *Angew. Chem., Int. Ed.*, 2017, **56**, 5812–5816.
39 C. Xu, H. Li and B. Yin, *Biosens. Bioelectron.*, 2015, **72**, 275–281.
40 H. Zhang, C. Wang, G. Wang, K. Wang and K. Jiang, *Biosens. Bioelectron.*, 2016, **78**, 344–350.
41 D. Gong, S.-C. Han, A. Iqbal, J. Qian, T. Cao, W. Liu, W. Liu, W. Qin and H. Guo, *Anal. Chem.*, 2017, **89**, 13112–13119.
42 B. Zhu, X. Zhang, Y. Li, P. Wang, H. Zhang and X. Zhuang, *Chem. Commun.*, 2010, **46**, 5710–5712.
43 X.-L. Liu, L.-Y. Niu, Y.-Z. Chen, M.-L. Zheng, Y. Yang and Q.-Z. Yang, *Org. Biomol. Chem.*, 2017, **15**, 1072–1075.
44 G.-J. Kim, K. Lee, H. Kwon and H.-J. Kim, *Org. Lett.*, 2011, **13**, 2799–2801.
45 S. Qi, W. Liu, P. Zhang, J. Wu, H. Zhang, H. Ren, J. Ge and P. Wang, *Sens. Actuators, B*, 2018, **270**, 459–465.
46 X. Han, X. Song, F. Yu and L. Chen, *Chem. Sci.*, 2017, **8**, 6991–7002.
47 X. Zhang, J.-Y. Liu, W.-W. Ma and M.-L. Yang, *J. Mater. Chem. B*, 2016, **4**, 6662–6669.
48 N. Karton-Lifshin, L. Albertazzi, M. Bendikov, P. S. Baran and D. Shabat, *J. Am. Chem. Soc.*, 2012, **134**, 20412–20420.
49 M. J. Frisch, *et al.*, *Gaussian 09, Revision C.01*, Gaussian Inc., Wallingford, CT, 2010.
50 X. Zhang and J.-Y. Liu, *Dyes Pigm.*, 2016, **125**, 80–88.

